Drop Oscillation Modeling

Lev Shchur[1,2(✉)] and Maria Guskova[1,2]

[1] Landau Institute for Theoretical Physics, Chernogolovka, Russia
lev@landau.ac.ru
[2] National Research University Higher School of Economics, Moscow, Russia
{lshchur,mguskova}@hse.ru

Abstract. The classical problem of oscillations of liquid droplets is a good test for the applicability of computer simulation. We discuss the details of our approach to a simulation scheme based on the Boltzmann lattice equation. We show the results of modeling induced vibrations in a chain of three drops in a closed tube. In the initial position, the central drop has formed as an ellipsoid, out of the spherical equilibrium form. The excitation of vibrations in the left and right droplets depends on the viscosity of the surrounding fluid and the surface tension. Droplets are moving out of the initial position as well. We discuss the limits of the applicability of our model for the study of such a problem. We will also show the dynamics of the simulated process.

Keywords: Lattice Boltzmann Method · Computer simulations · Drop oscillations · Surface tension · Viscosity · Hybrid computing architecture CPU/GPGPU

1 Introduction

The collective motion of the drops in the liquid confined in the complex geometry is a challenging problem of the supercomputer simulations. The interest is two-fold. Firstly, there are many applications in the manufacturing [1], printing [2], oil recovery [3], and cyber-physical [4] systems, among many others. Secondly, it is crucial for the simulations of the flows in the veins connected with the exact drug delivery [5] or problems of tumor cells spreading [6].

Lattice Boltzmann method (LBM) [7] is suitable for the simulation of multicomponent fluid in the complex environment [8]. The LBM is a linear method and can be easily partitioned in space and can be realized in the very efficient massively parallel simulations using supercomputer capabilities.

In the paper, we report the effect of the eigenfrequencies on the collective motion. We simplify the problem and choose the minimal setup of three drops with similar properties, and analyze the drop swing and movement of the drops influenced by the oscillation of another drop. Oscillations originated because of the initial form of one of the drops. We use the symmetric set up with the three drops of the same size and properties immersed in another fluid. At the

initial time, the central drop excited in the eigenfrequency oscillation having the ellipsoid form while another two drops (placed at the left and right sides) are in the non-excited state, i.e., with the spherical shape. The volumes of all three drops are the same. The development of the oscillations and movement does depend on the fluid viscosity and surface tension. The simulation shows that the side drops first squeezed and then starts moving out of the center. This effect can initiate the instability of the chain of the drops in the experiment [9].

Simulations based on the Palabos development platform [10] and performed with MPI on the supercomputer cluster.

The LBM method used in simulations is described briefly in Sect. 2. The geometry and parameters of simulations are given in Sect. 3. Section 4 give some details of the program code and computations. Simulations presented in the Sect. 5 and discussion of results is presented in the Sect. 6.

2   Lattice Boltzmann Equations

We use the Shan–Chen method for multiple component fluid flows [11]. The time and three-dimensional space (D3) is discrete and measured in units of Δt and Δx, correspondingly. We use three dimensional D3Q27 representation of 27 velocities c_i pointing from the center of the cube to 8 vertices, to the middle of 12 edges, and to the middle of 6 faces, and to 1 center (zero velocity), i.e. $i = 0, 1, 2, \ldots, 26$ (see, f.e., Refs. [12] and [13]). Distribution functions are defined $f_i^j(\boldsymbol{x}, t)$ for all 27 velocities c_i and for each of two components of fluid ($j = 1, 2$) at lattice position $\boldsymbol{x}$ and evaluated in time by the equations

$$f_i^j(\boldsymbol{x} + \boldsymbol{c}_i \Delta t, t + \Delta t) - f_i^j(\boldsymbol{x}, t) = \Omega_i^j(f) + S_i^j, \tag{1}$$

with the collision operator $\Omega_i^j(\boldsymbol{x}, t)$. The collision term $S_i^j = \boldsymbol{F}^j \cdot \boldsymbol{c}_i$ controls the strength of the interaction potential between fluid components $\{j\}$, the force F^j is defined through the Shan–Chen potential [11]. Collision operator is written in the BGK form [14]

$$\Omega_i^j(f) = -\frac{f_i^j - \tilde{f}_i^j}{\tau} \Delta t, \tag{2}$$

with equilibrium distribution function [13]

$$\tilde{f}_i^j(\boldsymbol{x}, t) = \mathrm{w}_i \rho^j(\boldsymbol{x}, t) \left(1 + \frac{\boldsymbol{u} \cdot \boldsymbol{c}_i}{c_s^2} + \frac{(\boldsymbol{u} \cdot \boldsymbol{c}_i)^2}{2c_s^4} - \frac{\boldsymbol{u} \cdot \boldsymbol{u}}{2c_s^2}\right), \tag{3}$$

where sound speed $c_s = \Delta x / (\Delta t \sqrt{3})$.

3   Physical Setup

Three drops are placed in the box of linear sizes 500, 250, and 250 in the directions x, y, and z, correspondingly. The centers of the drops are in the initial positions: the left drop $x_l, y_l, z_l = 175, 125, 125$, the central drop $x_c, y_c, z_c =$

$250, 125, 125$, the right drop $x_r, y_r, z_r = 325, 125, 125$. All drops have the same volume of $4/3\pi R^3$ with $R = 30$. At the first moment, the right and left drops are the spheres, and the central drop is the ellipsoid with the z-axes enlarged to $2R$ while keeping the same volume.
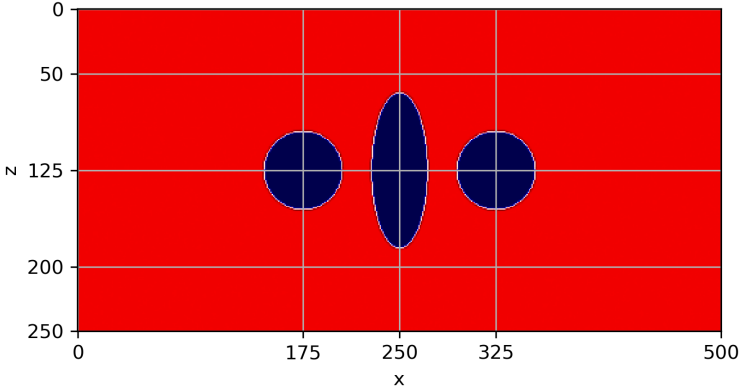

Fig. 1. Cross-section of the initial state of the drops, $y = 125$.

Leaving alone, the central drop with the initial ellipsoid state will oscillate with the component $n = 2$ of the eigenfrequency, according to the Rayleigh formula [15, 16]

$$\omega_2^2 = \frac{24}{3\rho_D + 2\rho_F} \frac{\sigma}{R^3},\qquad(4)$$

where σ is the surface tension, and ρ_D and ρ_F is the density of the drop and the surrounding fluid. In simulations, the period of oscillations is about $1000\Delta t$ with the relaxation parameter $w = 4/3$, and oscillations practically damped after 2–3 periods. The details of the single drop oscillation presented in the paper [17].

In the following, we are interested in the orchestrated oscillations of all three drops caused by the swing of the central drop with the initial state exciting the frequency (4). The cross-section at $y = 125$ of the initial state of the simulations is presented in the Fig. 1.

The density ρ_D (equivalent to ρ^1 in the Expr. (1)) of the fluid component inside the drop is set as unity with the small excess $\rho_D = 1.01$, and the density of the surrounding fluid ρ_F (equivalent to ρ^2 in the Expr. (1)) is set as unity with the small excess $\rho_D = 1.01$, and the initial velocities are set up to zero. The collision constant $G = 2.7$ controls the interface region of two fluids [13]. Both fluids have the equal parameters of the viscosity ν associated with the values of the relaxation parameter $w_1 = w_2 = w = 1/\tau$

$$\nu = c_s^2 \left(\frac{1}{w} - \frac{\Delta t}{2} \right).\qquad(5)$$

Simulations have been performed for the number of viscosity values, see the Table 1.

Table 1. Values of the viscosity ν and associated values of the relaxation parameter w used in simulations, see Expr. (5)

w	16/11	4/3	100/77	200/157	400/317	16/13
ν	0.625	0.083	0.090	0.095	0.0975	0.104

4   Computational Details

Program code is based on the Palabos C++ development platform [10]. Data defined through classes of type MultiBlock, which are the 3-dimensional matrices in our case. MultiBlockLattice3D data structure defines a Lattice Boltzmann cell, with double-precision floating-point numbers. Each cell contains 27 distribution functions. Calculation of the left part in Exp. (1) is named streaming, and calculation of the first term in the right part is called a collision. Computations of the streaming and the BGK collision are local, and all twenty-seven functions f_i can be computed in parallel. Technically, we solve two sets of the LBM Eqs. (1–3), one for the fluid inside the drop and another one for the fluid outside the drop. Each fluid represented by the own MultiBlockLattice data structure. Therefore the streaming process in the left part Expr. (1) and collision with the operator (2) can be calculated in parallel for each of the fluids. The data processor calculates the Shan-Chen collision dynamics between two fluids as the second term in the right part of Expr. (1). This is a non-local operation, and this part of computations avoid the parallelization. The local properties of the BGK collision and of the distribution function streaming allows the additional possibility for parallelization – the lattice partitioning in the space.

Both fluids exist in the whole domain of simulations, and each fluid represented by 250 by 250 by 500 cells. Those fluid associated with the drop has a normal density $\rho_D = 1.01$ inside the drop and negligible density 0.0001 outside the drop. Contrary, the density of surrounding fluid has density $\rho_F = 1.01$ outside the drop and negligible density 0.0001 inside the drop. The time of the life for the drop with such a density gradient is order of magnitude larger than the total simulation time.

The parallel implementation uses MPI with the library MPICH version 3.2.1 [18]. The simulations in the next section have been done using Intel Xeon Gold 6152 2.1 GHz CPU with onboard memory DDR4 2.666 GHz 768 GB RAM. The program saves the whole computation field to the hard-disk every fifty steps of time, and it takes about 125 sec for this cycle at 22 CPU cores.
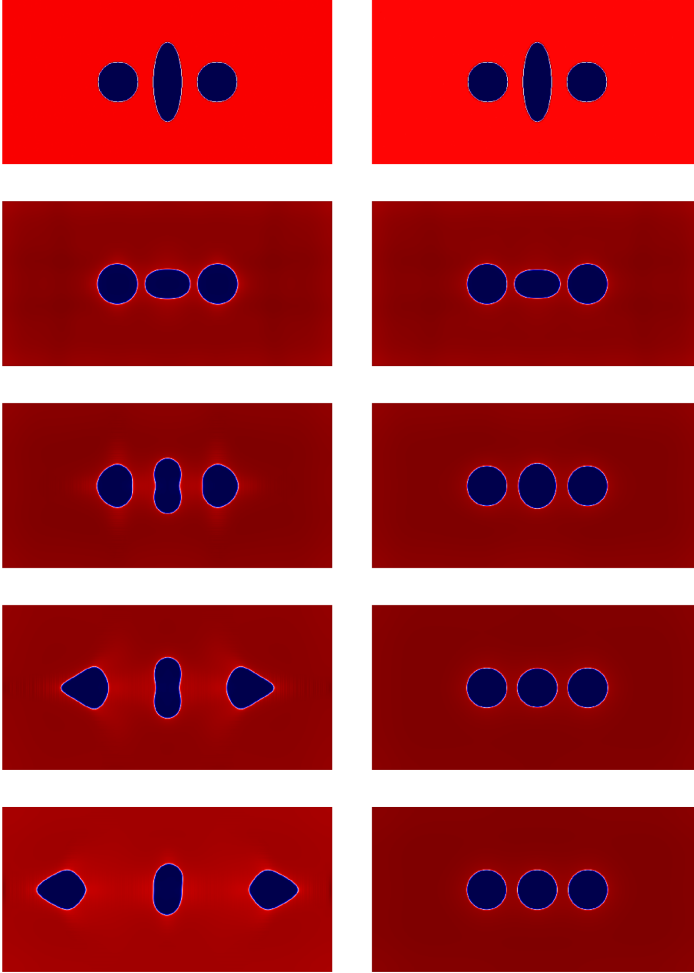
Fig. 2. Cross-section of the drops, $y = 125$ at the value of viscosity $\nu \approx 0.083$ (the left column) and $\nu \approx 0.104$ (the right column) at different times, measured in the units $\Delta t = 1$, from top to bottom $t = 50, 1000, 2000, 3000,$ and 4000. The axis are the same as in Fig. 1.

5   Drop Chain Movement

There are experiments (see, f.e., the review [9]) in which the chain of equidistantly injected drops can occasionally break the order. In some cases, one of the drops goes out of the chain. Our idea is that the broke of the symmetry in the chain can be attributed to some imperfection in the drop form at the moment of injection. This imperfection will trigger the oscillations of the drop, which should follow to the spectrum of the Rayleigh frequencies [15]. The idea is to check can the oscillations in one of the drops influence the others or not. The most simple

question of that kind is how the oscillations of the central drop have influenced on the left and right drops? We perform simulations of three drops to answer the question.

We simulate the three drops behavior for the number of viscosities shown in the Table 1, and for the same initial conditions formulated in the Sect. 3. Figure 2 shows the dynamics of the drops for two typical cases, $\nu = 0.083$ and $\nu = 0.104$, and which can be considered as "low" and "high" viscosities in the drop dynamics. Note that the difference in the viscosities is only 20%, and it turns quite enough for the observation of two quite different behavior.

The left column in Fig. 2 demonstrates the dynamics of the drops at the lower viscosity, $\nu = 0.083$, as the snapshot at the number of time moments. The top figure shows drops at the very beginning step, $t = 50$; the next figure is taken at the time $t = 1000$, close to the half-period of oscillation [17]. Oscillation is damped by viscosity, and drop also elongates in the perpendicular to the figure direction, keeping the volume constant. At that time, there is no visible distortion of the side drops. At the next figure corresponding to approximately the full period of ω_2-oscillations of the free drop, one can see the apparent effect of the hydrodynamic interactions. The left and right drops squeezed at the sides close to the center; in addition, drops start to sharpen the outer sides due to the internal movement of fluid inside the drops. It is visible that the central drop is no more in the ω_2 regime as the higher mode of oscillations is already present at the time $t = 2000$. The central drop forms the dumbbell-like form due to the reflection of the surrounding fluid from the side drops. It is interesting that about the same time, the new phenomena visible in the figures in the left column in Fig. 2, it is the flow of the drops out of the center. The flow consists of the complicated excitations, with the conic form closer to the box, and with the movement of the center of mass of the left and right drops toward the boundary.

The last two bottom figures in Fig. 2 show the movement of the side drops out of the center one, with the sharp conic form of the outer sides. We have to mention here that we use bounce-back boundary conditions at the box, and there are reflections of the waves in the surrounding fluid because of that. There is a reflection of the drop from the boundary at the time ≈ 3700 (not shown in the figure). We should one more time to notice that due to the symmetry, the right drop has the same behavior as the left one.

The observed effects seem to depend on the viscosity as one can see from the right column of figures in Fig. 2, where initial oscillations with the frequency ω_2 does not visibly influence the right and left drops. The oscillation of the central drop is dumped almost entirely by viscosity on the simulated time scale. One can see that in contrast to the left column of figures with the lower viscosity, there is no visible excitation of the higher modes, and central drop have the ellipsoid form at the time of the full period $t = 2000$.

Finally, at the bottom figure, drops seem to form an equilibrium picture with the drops of equal radii R and with the distance between drops close to $R/2$. Nevertheless, the visible equilibrium is not the final stage of the dynamics. One should look for longer times.

We present in the Fig. 3 the position of the left side of the left drop for the number of values of the relaxation parameter w (consult the Table 1 for the corresponding values of viscosities). Indeed, while simulate drops at the relaxation parameter $w = 16/13$, which corresponds to the right column of figures in the Fig. 2 father in time, the left side of the left drop is starting moving to the left. It is not surprising, however, taking into account the friction properties of the fluid [19].
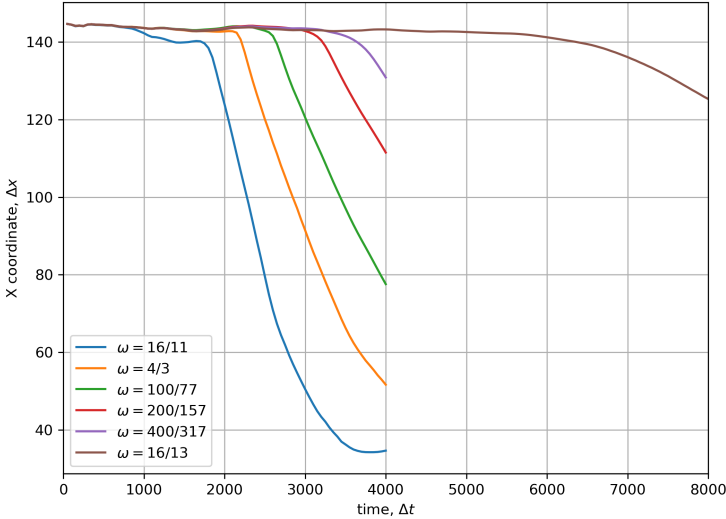

Fig. 3. The time dependence of the left side of the left drop for the different values of the fluid viscosity.

6   Conclusion

Simulations demonstrate the dynamics of the drop chain while exiting oscillations in one of the drops. The level of excitations does depend on the fluid viscosity, which can trigger the visible distortion of other drops, or not. Anyway, some drop movement can be visible at the longer observation times for the large values of viscosities.

We present computer simulation of the oscillations of three drops, with the central drop is in the first exited ellipsoid state, and the left and right drops initially rest in the spherical states. We simulate the system in the box with the bounce-back boundary conditions, and we found the influence of the boundaries is not essential for the most time of simulations. We found the visible excitations of the left and right drops, and even excitation of the higher harmonic of the central drop for the small enough fluid viscosity. For the significant values of

the viscosity, there is relatively fast dumping of the central drop oscillations and no visible excitation of the neighboring drops. The developed setup can be used for the simulation of the movement of the long chain of drops in the channel in order to explain the instability of the chains observed in the experiments [9].

We also find that symmetry of the drop chain against the boundaries may influence the dynamics at the longer observation times. We use an even number of cells in all directions. Therefore the center of the central drop is not in the middle of the box, and reflections from the bounce-back boundaries lead to the attractive force in the diagonal direction. To avoid that, we check the dynamics in the box with an odd number of cells. We found there are no attractive forces from the boundaries in that case.

We also check the possible influence of the level of the velocity discretization, the D3Q19 model, with 19 velocities. We do not find any visible difference at the time of the dynamic observation.

References

1. Simonelli, M., et al.: Towards digital metal additive manufacturing via high-temperature drop-on-demand jetting. Addit. Manuf. **30**, 100930 (2019)
2. Ben-Barak, I., et al.: Drop-on-Demand 3D printing of lithium iron phosphate cathodes. J. Electrochem. Soc. **166**, A5059 (2019)
3. Yuan, D., Moghanloo, R.G.: Nanofluid pre-treatment, an effective strategy to improve the performance of low-salinity waterflooding. J. Petrol. Sci. Eng. **165**, 978 (2018)
4. Ibrahim, M., Chakrabarty, K., Zeng, J.: BioCyBig: a cyberphysical system for integrative microfluidics-driven analysis of genomic association studies. IEEE Trans. Big Data (2016). https://doi.org/10.1109/TBDATA.2016.2643683
5. Esmaeili, S.: An artificial blood vessel fabricated by 3D printing for pharmaceutical application. Nanomed J. **6**, 183 (2019)
6. Freitas, V.M., Hilfenhaus, G., Iruela-Arispe, M.L.: Metastasis of circulating tumor cells: speed matters. Dev. Cell **45**, 3 (2018)
7. Succi, S.: The Lattice Boltzmann Equation: For Complex States of Flowing Matter. Oxford University Press, Oxford (2018)
8. Shan, X., Doolen, G.: Multicomponent lattice-Boltzmann model with interparticle interaction. J. Stat. Phys. **81**, 379 (1995)
9. Beatus, T., Bar-Ziv, R.H., Tlusty, T.: The physics of 2D microfluidic droplet ensembles. Phys. Rep. **512**, 103 (2012)
10. Latt, J., et al.: Palabos: Parallel Lattice Boltzmann Solver. Comput. Math. Appl. (2020, in Press). https://doi.org/10.1016/j.camwa.2020.03.022

11. Shan, X., Chen, H.: Lattice Boltzmann model for simulating flows with multiple phases and components. Phys. Rev. E **47**, 1815 (1993)
12. Suga, K., Kuwata, Y., Takashima, K., Chikasue, R.: A D3Q27 multiple-relaxation-time lattice Boltzmann method for turbulent flows. Comput. Math. Appl. **69**, 518 (2015)
13. Krüeger, T., Kusumaatmaja, H., Kuzmin, A., Shardt, O., Silva, G., Viggen, E.M.: The Lattice Boltzmann Method, Principles and Practice. Springer, Cham (2017)
14. Bhatnagar, P.L., Gross, E.P., Krook, M.: A model for collision processes in gases. I. Small amplitude processes in charged and neutral one-component systems. Phys. Rev. **94**, 511 (1954)
15. Rayleigh, L.: On the capillary phenomenon of jets. Proc. R. Soc. London **29**, 71 (1879)
16. Lamb, H.: Hydrodynamics. Dover, New York (1932)
17. Guskova, M., Shchur, V., Shchur, L.: Simulation of drop oscillation using the lattice Boltzmann method. Lobachevskii J. Math. **41**(6), 992–995 (2020)
18. https://www.mpich.org/2017/11/11/mpich-3-2-1-released/
19. Landau, L.D., Lifshitz, E.M.: Course of Theoretical Physics VI: Fluid Mechanics. Pergamon Press, Oxford (1982)